



**University of  
Zurich<sup>UZH</sup>**

**Zurich Open Repository and  
Archive**

University of Zurich  
University Library  
Strickhofstrasse 39  
CH-8057 Zurich  
[www.zora.uzh.ch](http://www.zora.uzh.ch)

---

Year: 2009

---

## **An exact accelerated stochastic simulation algorithm.**

Mjolsness, E ; Orendorff, D ; Chatelain, P ; Koumoutsakos, P

**Abstract:** An exact method for stochastic simulation of chemical reaction networks, which accelerates the stochastic simulation algorithm (SSA), is proposed. The present "ER-leap" algorithm is derived from analytic upper and lower bounds on the multireaction probabilities sampled by SSA, together with rejection sampling and an adaptive multiplicity for reactions. The algorithm is tested on a number of well-quantified reaction networks and is found experimentally to be very accurate on test problems including a chaotic reaction network. At the same time ER-leap offers a substantial speedup over SSA with a simulation time proportional to the 23 power of the number of reaction events in a Galton-Watson process.

DOI: <https://doi.org/10.1063/1.3078490>

Posted at the Zurich Open Repository and Archive, University of Zurich

ZORA URL: <https://doi.org/10.5167/uzh-39542>

Journal Article

Originally published at:

Mjolsness, E; Orendorff, D; Chatelain, P; Koumoutsakos, P (2009). An exact accelerated stochastic simulation algorithm. The Journal of chemical physics, 130(14):144110.

DOI: <https://doi.org/10.1063/1.3078490>

# An exact accelerated stochastic simulation algorithm

Eric Mjolsness,<sup>1,a)</sup> David Orendorff,<sup>1</sup> Philippe Chatelain,<sup>2</sup> and Petros Koumoutsakos<sup>2</sup>

<sup>1</sup>*Department of Computer Science, University of California, Irvine, U.C. Irvine, California 92697, USA*

<sup>2</sup>*Computational Science, ETH Zürich, CH-8092 Zurich, Switzerland*

(Received 16 June 2008; accepted 15 January 2009; published online 13 April 2009)

An exact method for stochastic simulation of chemical reaction networks, which accelerates the stochastic simulation algorithm (SSA), is proposed. The present “ER-leap” algorithm is derived from analytic upper and lower bounds on the multireaction probabilities sampled by SSA, together with rejection sampling and an adaptive multiplicity for reactions. The algorithm is tested on a number of well-quantified reaction networks and is found experimentally to be very accurate on test problems including a chaotic reaction network. At the same time ER-leap offers a substantial speedup over SSA with a simulation time proportional to the  $2/3$  power of the number of reaction events in a Galton–Watson process. © 2009 American Institute of Physics.

[DOI: [10.1063/1.3078490](https://doi.org/10.1063/1.3078490)]

## I. INTRODUCTION

The stochastic simulation algorithm<sup>1</sup> (SSA) is a widely used method for simulating the stochastic dynamics of chemical reaction networks. SSA executes every reaction event and provides an accurate view of the system dynamics, albeit at a significant computational cost over the corresponding mass-action differential equations that approximate the mean numbers of each molecular species. A number of algorithms have been proposed for the acceleration of the SSA at the expense of its accuracy. The  $\tau$ -leaping algorithm<sup>2</sup> and its recent variants<sup>3–5</sup> simulate leaps over several reaction events during a preselected time increment. Further developments include multiscale SSAs such as “nested stochastic simulation,”<sup>6</sup> the multiscale methods,<sup>7,8</sup> and the “slow-scale stochastic simulation” algorithm.<sup>9</sup> Another acceleration method<sup>10</sup> uses rejection sampling to achieve constant time scaling with the number of reaction channels; this differs from the present work which uses rejection sampling to improve scaling with respect to the number of reaction events.

A related work is the *R-leaping* algorithm<sup>11</sup> which proposes the simulation of preselected numbers of reaction firings that occur over time intervals sampled from an Erlang distribution. An essential aspect of these approximate methods is the requirement that the changes to the reaction rate or “propensity” functions are small during each step.

We present a SSA which, similar to *R-leap*, accelerates SSA by executing multiple reactions per algorithmic step, but which samples the reactant trajectories from the same probability distribution as the SSA. This “exact *R-leap*” or “ER-leap” algorithm is a modification of the *R-leap* algorithm which is both exact and capable of substantial speedup over SSA. The simplest versions of both  $\tau$ -leap and *R-leap* have difficulties with the potential of producing negative numbers of reactants, which can be fixed by modifications such as binomial tau-leap<sup>3</sup> and modified tau-leap.<sup>4</sup> Since ER-

leap is exact, it intrinsically avoids this potential pitfall; stochastic moves to negative reactant states have zero probability and will be rejected. We demonstrate by computational experiments that ER-leap can execute in time sublinear in the number of reaction events to be simulated, while remaining exact. The algorithm is based on the rejection sampling concept, using efficiently computable bounds on the SSA probability distribution.

The paper is organized as follows. In Sec. II we derive upper and lower bounds on the SSA reaction probabilities after multiple reactions, expressed using matrix notation for Markov processes, and use rejection sampling to derive the ER-leap algorithm. The algorithm itself is stated, analyzed for cost, and illustrated in Sec. II E. In Sec. III we report on a series of numerical experiments designed to evaluate the accuracy and speedup of the ER-leap algorithm. In Sec. IV we discuss the results and conclude with an assessment of the method in the context of related works and an outline of directions for future work.

## II. THEORY

This section is organized as follows. Sections II A–II C introduce the required notations, reaction probabilities, and bounds on these probabilities, respectively. The ER-leap algorithm’s key update equations are derived from these probability bounds in the calculations of Sec. II D. The resulting algorithm is assembled from the key update equations, analyzed for cost, and illustrated in the case of a simple reaction network in Sec. II E.

We consider a set of reactions, indexed by  $r$ , among chemical species  $C_a$ , indexed by  $a$ ,

$$\{m_a^r C_a\} \rightarrow \{m_a'^r C_a\}, \quad \text{with reaction rate } \rho_r. \quad (1)$$

Here  $\mathbf{m}^r = [m_a^r]$  and  $\mathbf{m}'^r = [m_a'^r]$  are the input and output stoichiometries of the reaction  $r$ . In the following we derive an expression for the probability of states after a number of such reaction events.

<sup>a)</sup>Electronic mail: [emj@uci.edu](mailto:emj@uci.edu). Also at Institute of Genomics and Bioinformatics.

## A. Notations

We introduce the following notations. The definition of a version of the indicator function  $\mathbf{1}$  from Boolean values to integers is

$$\mathbf{1}(P) \equiv \begin{cases} 1 & \text{if predicate } P \text{ is true} \\ 0 & \text{otherwise.} \end{cases}$$

The Kronecker delta function  $\delta(a, b)$  or  $\delta(a - b)$  is

$$\delta(a - b) = \delta_{ab} = \mathbf{1}(a = b) = \begin{cases} 1 & \text{if } a = b \\ 0 & \text{otherwise.} \end{cases}$$

The function  $V = \text{diag}(\mathbf{v})$  turns a  $d$ -dimensional vector  $\mathbf{v}$  into a  $d \times d$  square matrix  $V$  with components  $V_{ij} = \delta_{ij}v_i$ , i.e., zero everywhere except the diagonal which contains the components of  $\mathbf{v}$ . Given an ordered list of noncommuting matrices  $V^{(k)}$  indexed by integers  $k$ , we define the ordered product notation

$$\prod_{k=K_{\max} \searrow K_{\min}} V^{(k)} = V^{(K_{\max})} \cdot V^{(K_{\max}-1)} \cdot \dots \cdot V^{(K_{\min}+1)} \cdot V^{(K_{\min})}.$$

In addition to the standard set-builder notation  $\{x | P(x)\}$  for defining the members of a set from a predicate  $P$ , we will build ordered sets or lists in a similar way using square brackets:  $[x(i) | P(x(i), i) | i \in \mathcal{I}]$  imposes the image of a pre-existing ordering on the index set  $\mathcal{I}$  (such as the ordering of natural numbers if  $\mathcal{I} \subseteq \mathbb{N}$ ) onto any elements  $x(i)$  selected for inclusion by the optional predicate  $P$ , and thus denotes a set together with a total ordering. For example, the B-tuple  $[n_b | b \in \{1, \dots, B\}]$  denotes the components of a vector  $\mathbf{n}$ .

## B. Markov chain and multireaction probabilities

We denote states of the chemical reaction network by  $I, J, K$ , time by  $t$ , and algorithm step number by  $k$ . Let  $n_a$  be the number of reactant molecules of type  $a$  present in a given state  $I$  at time  $t$ , so that  $I$  corresponds to the vector or ordered list of non-negative integers  $\mathbf{n} = [n_b | b \in \{1, \dots, B\}]$ . Likewise if we are discussing several such states that are present at different times  $t'$  and  $t''$ , we may denote them by  $\mathbf{n}'$  and  $\mathbf{n}''$  or correspondingly by  $J$  and  $K$ . The time interval between successive reactions is denoted by  $\tau$ .

We wish to track the time evolution of the probabilities  $\text{Pr}(I, t)$ , for all possible system states  $I$  by employing the governing master (or Chapman–Kolmogorov) equation,<sup>12</sup> which we shall use here. We define  $\text{Pr}(I, t | J, k)$  as the “just-reacted state probability:” the probability of being in state  $I$  at time  $t$  immediately after the  $k$ th reaction event, given that the state is  $J$  at time zero. The Chapman–Kolmogorov equation<sup>12</sup> for such just-reacted state probabilities follows from taking  $k$  to be a discrete time coordinate and can be written<sup>13</sup>

$$\text{Pr}(I, t | J, K) \approx \sum_K \int_0^t d\tau \text{Pr}(I, \tau | K, 1) \text{Pr}(K, t - \tau | J, k - 1). \quad (2)$$

A key quantity in this equation is the “kernel”  $\text{Pr}(I, \tau | K, 1)$ : the probability that if  $k=1$  reaction event has just occurred, and if the previous state was  $K$ , then a time  $\tau$  has elapsed

since the last reaction event and the new state is  $I$ . This kernel also provides the linear weights that advance the quantity  $\text{Pr}(K, t - \tau | J, k - 1)$ , which is the probability distribution over states  $K$  just after  $k-1$  reactions to produce the probability distribution over states  $I$  after  $k$  reactions,  $\text{Pr}(I, t | J, k)$ . So we can rename this kernel the conditional distribution,

$$\mathcal{W}(I, t' | J, t) = \text{Pr}(I, t' - 1 | J, 1),$$

using notation similar to that of Ref. 13. This  $\mathcal{W}$  is analogous to a matrix with two indices, each of which is a pair consisting of a discrete-valued systems state (such as  $I$  or  $J$ ) and a continuous-valued time (such as  $t'$  or  $t$ ).

Under the SSA algorithm  $\mathcal{W}$  must factor into an update from time  $t$  to  $t'$  and then from state  $J$  to state  $I$ ,

$$\mathcal{W}(I, t' | J, t) \approx \hat{W}_{I,J} \exp(-(t' - t)D_{JJ}) \mathbf{1}(t' \geq t), \quad (3)$$

with

$$D = \text{diag}(\mathbf{h} \cdot \hat{W}), \quad (4)$$

where  $\mathbf{h}$  is the vector whose components are all 1 and “diag” turns a vector into the corresponding diagonal matrix. This result is derived in more detail in Refs. 14 and 13. The state space transition matrix  $\hat{W}$  contains the summed probability rates or “propensities” for all reactions that could move the system from state  $J$  to state  $I$ . The exponential term governs the distribution of waiting times between reaction events, as in the SSA<sup>3-5</sup> and R-leap<sup>11</sup> algorithms. The  $I$ th component of the vector  $\mathbf{h} \cdot \hat{W}$ , which is defined as  $D_{II}$ , is the total probability per unit time for the system to leave state  $I$ . [In many papers the summed reaction rate  $D_{II}$  is denoted as  $a_0(\mathbf{n})$  instead.]

Continuing with the matrix analogy for  $\mathcal{W}$ , and assuming that  $t < 0 \wedge k \geq 0 \Rightarrow \text{Pr}(I, t | J, k) = 0$ ,

$$\text{Pr}(I, t | J, k) \approx \sum_K \int_{-\infty}^{\infty} d\tau \mathcal{W}(I, t | K, t - \tau) \text{Pr}(K, t - \tau | J, k - 1). \quad (5)$$

Using vector notation  $\text{Pr}(\cdot | J, k)$  for the  $(I, t)$  parameters, we may write

$$\text{Pr}(\cdot | J, k) \equiv \mathcal{W} \circ \text{Pr}(\cdot | J, k - 1), \quad (6)$$

where the matrix-vector inner product  $\circ$  is both a sum over states and an integral over all times  $t$ , as in Eq. (5), and where

$$\mathcal{W} = \hat{W} \exp(-\Delta t D) \mathbf{1}(\Delta t \geq 0). \quad (7)$$

Equation (7) expresses the Markov chain for the change in both chemical state and total time, after one reaction event. The matrix  $\hat{W}$  contains probability rates or propensities, the much larger matrix  $\mathcal{W}$  contains only normalized probability densities for the combination of a discrete state change and a continuous time change  $\Delta t$ .

From Eqs. (6) and (7), after  $k$  reaction events,

$$\begin{aligned}\Pr(\cdot|J,k) &= \mathcal{W}^k \circ \Pr(\cdot|J,0) \\ &= [\hat{W} \exp(-\Delta t D) \mathbf{1}(\Delta t \geq 0)]^k \circ \Pr(\cdot|J,0).\end{aligned}\quad (8)$$

This expression is in accord with, for example, Theorem 10.1 of Ref. 14.

The aim of the SSA algorithm is to sample from the distribution  $\Pr(I, t|J, k)$ . Equation (6) may be taken as a concise statement of a single SSA algorithm update: it is a product of two conditional distributions, one ( $\hat{W}D^{-1}$ ) for molecular state  $I$  given state  $J$ , and another one which samples time  $t'$  given time  $t$  and state  $J$  according to conditional distribution  $D \exp(-\Delta t D) \mathbf{1}(\Delta t \geq 0)$ , evaluated at state  $J$ . These two sampling steps are alternated and iterated  $k$  times as in Eq. (8).

To derive  $D$  and  $\mathcal{W}$ , and therefore [by Eq. (7)] the detailed SSA simulation process, we need only define the matrix  $\hat{W}$  of probability rates for a chemical reaction network. For the reaction network of Eq. (1), defining the net stoichiometry

$$\Delta m_a^r = m_a'^r - m_a^r,$$

the usual mass-action assumption for stochastic reactions corresponds to

$$\hat{W}(\mathbf{n}'|\mathbf{n}) = \sum_r \hat{W}^{(r)}(\mathbf{n}'|\mathbf{n}) \quad \text{and} \quad \hat{D}(\mathbf{n}'|\mathbf{n}) = \sum_r \hat{D}^{(r)}(\mathbf{n}'|\mathbf{n}),$$

where the probability rate matrix  $\hat{W}^{(r)}$  for reaction  $r$  has elements given by a product of factors for all the input reactants (all  $a$  for which  $m_a^r \neq 0$ ) times a product of Kronecker delta functions that enforce the net stoichiometries on the system state,

$$\hat{W}_{\mathbf{n}',\mathbf{n}}^{(r)} = \rho_r \left( \prod_{\{a|m_a^r \neq 0\}} \frac{n_a!}{(n_a - m_a^r)!} \right) \left[ \prod_{\{a|\Delta m_a^r \neq 0\}} \delta(n_a' - n_a - \Delta m_a^r) \right],$$

the corresponding diagonal matrix  $D^{(r)}$  is

$$D^{(r)}(\mathbf{n}'|\mathbf{n}) = \rho_r \left( \prod_{\{a|m_a^r \neq 0\}} \frac{n_a!}{(n_a - m_a^r)!} \right) \left[ \prod_{\{a|\Delta m_a^r \neq 0\}} \delta(n_a' - n_a) \right].$$

(The elements of  $\hat{W}^{(r)}$  are essentially reaction “propensity functions,” with a constant coefficient  $\Pi_a(1/(m_a^r!))$  that can be absorbed into the definition of  $\rho_r$  to maintain notational consistency with the law of mass action, as discussed in Sec. 3.4 of Ref. 15 which also uses notation similar to that used here.) If we define  $W = \hat{W} - D$ , SSA dynamics simulates trajectories<sup>12</sup> drawn from the solution to the master equation,  $dp/dt = W \cdot p$ .

### C. Upper and lower bounds

In order to derive a new simulation algorithm, equivalent to SSA, using rejection sampling,<sup>16</sup> we now seek simplified upper and lower bounds on the probability rate  $\hat{W}_{I,J}^{(r)} \exp(-\Delta t D_{JJ})$  [from Eq. (7)] for a single reaction event. However, we will assume that the reaction event to be bounded occurs within a run of  $L$  events in the SSA algorithm, in order to execute  $L$  reactions at once in the manner

of the R-leap algorithm.<sup>11</sup> As we will see, this essentially comes down to bounding each combinatorial factor  $n_a!/(n_a - m_a^r)!$  with a constant bound, even though it may change throughout the run of  $L$  events.

For step number  $l$  within the run we must find a simplifying upper bound for the key expression

$$F_n^{(r)} \equiv \prod_{\{a|m_a^r \neq 0\}} \left( \begin{cases} \frac{n_a!}{(n_a - m_a^r)!} & \text{if } n_a \geq m_a^r \\ 0 & \text{otherwise} \end{cases} \right)$$

that occurs in  $\hat{W}$  and  $D$ , and also to find a simplifying lower bound for its contribution to  $D$ , in order to lower-bound both factors in  $\mathcal{W}$  under Eq. (3). The products  $\rho_r F_n^{(r)}$  are usually called propensity functions denoted  $a_r(\mathbf{n})$  for all  $R$  reaction channels,

$$\begin{aligned}a_r(\mathbf{n}) &\equiv \rho_r F_n^{(r)}, \\ a_0(\mathbf{n}) &\equiv \sum_{r=1}^R a_r(\mathbf{n}),\end{aligned}\quad (9)$$

possibly with a different normalization convention as a function of  $m_a^r$  if  $m_a^r \neq 1$  as mentioned in the previous section. In this work it is more convenient to keep separate the structural terms  $F_n^{(r)}$  and the reaction rates  $\rho_r$ , rather than combining them as in Eq. (9). Fortunately every  $F_n^{(r)}$  is monotonic in each  $n_a$ , so we may find upper and lower bounds on  $F_n^{(r)}$  by finding upper and lower bounds on each  $n_a$ .

A very simple, although not very tight, set of bounds is

$$n_a + l \min_r \{\Delta m_a^r\} \leq n_a' \leq n_a + l \max_r \{\Delta m_a^r\}.\quad (10)$$

The corresponding upper and lower bounds  $\tilde{F}_{IJ}$  and  $\underline{F}_{IJ}$  on  $F$  for the  $(l+1)$ -st first reaction event (after  $l$  reaction events have already occurred) within a run of  $L$  events is

$$\underline{F}_{\mathbf{n},l}^{(r)} \leq F_{\mathbf{n}'}^{(r)} \leq \tilde{F}_{\mathbf{n},l}^{(r)},$$

where

$$\begin{aligned}\underline{F}_{\mathbf{n},l}^{(r)} &\equiv F_{[n_a + l \min_r \{\Delta m_a^r\} | 1 \leq a \leq A]}^{(r)}, \\ \tilde{F}_{\mathbf{n},l}^{(r)} &\equiv F_{[n_a + l \max_r \{\Delta m_a^r\} | 1 \leq a \leq A]}^{(r)}.\end{aligned}\quad (11)$$

The sparsity structure of  $\hat{W}^{(r)}$  is given by  $S^{(r)} \in \{0, 1\}$ ,

$$\begin{aligned}\hat{S}_{\mathbf{n}',\mathbf{n}}^{(r)} &= \mathbf{1}(\hat{W}_{\mathbf{n}',\mathbf{n}}^{(r)} > 0) \in \{0, 1\} \\ &= \left( \prod_{\{a|m_a^r \neq 0\}} \mathbf{1}(n_a \geq m_a^r) \right) \left[ \prod_{\{a|\Delta m_a^r \neq 0\}} \delta(n_a' - n_a - \Delta m_a^r) \right],\end{aligned}$$

$$\hat{S}_{I,J} = \mathbf{1} \left( \sum_r S_{I,J}^{(r)} \right) = \mathbf{1}(\hat{W}_{I,J} > 0).$$

We will assume that reactions have unique outcomes (or redefine the states  $I$  so this becomes true),

$$\sum_I \hat{S}_{I,J}^{(r)} = 1. \quad (12)$$

Taking  $l$  consecutive steps of this chain results in another sparsity structure of “reachability,”

$$R_{l|Jl} \equiv (\hat{S}^l)_{I,J} = \mathbf{1}((\hat{W}^l)_{I,J} > 0) \equiv \begin{cases} 1 & \text{if } (\hat{W}^l)_{I,J} > 0 \\ 0 & \text{otherwise.} \end{cases}$$

We now start the reactions from state  $K=\mathbf{n}=[n_a||a \in \{1, \dots, A\}]$ . Since

$$\hat{W}_{\mathbf{n}',\mathbf{n}}^{(r)} = \rho_r F_{\mathbf{n}}^{(r)} \hat{S}_{\mathbf{n}',\mathbf{n}}^{(r)},$$

we have the bounds

$$R_{J|Kl} = 1 \Rightarrow \underline{W}_{I,J|Kl}^{(r)} \leq \hat{W}_{I,J}^{(r)} \leq \tilde{W}_{I,J|Kl}^{(r)},$$

where

$$\underline{W}_{I,J|K,l}^{(r)} \equiv \rho_r \underline{F}_{K,l}^{(r)} \hat{S}_{I,J}^{(r)},$$

$$\tilde{W}_{I,J|K,l}^{(r)} \equiv \rho_r \tilde{F}_{K,l}^{(r)} \hat{S}_{I,J}^{(r)}.$$

These quantities bound  $\hat{W}_{I,J}^{(r)}$ , in the circumstance that  $l$  reaction events have occurred since the system was in state  $K$ .

We also need to bound  $-D$  in Eq. (3). To this end, note from Eq. (4) that

$$D_{IJ} = \delta_{IJ} \sum_{I'} \sum_r \hat{W}_{I',J}^{(r)} = \delta_{IJ} D_{II}.$$

Then

$$\begin{aligned} R_{J|Kl} = 1 \\ \Rightarrow -\tilde{D}_{Kl} \\ = -\sum_r \sum_{I'} \tilde{W}_{I',J|Kl}^{(r)} \\ \leq -D_{JJ} \leq -\sum_r \sum_{I'} \underline{W}_{I',J|Kl}^{(r)} = -\underline{D}_{Kl}, \end{aligned}$$

where

$$\begin{aligned} \underline{D}_{Kl} &\equiv \sum_r \rho_r \underline{F}_{K,l}^{(r)}, \\ \tilde{D}_{Kl} &\equiv \sum_r \rho_r \tilde{F}_{K,l}^{(r)}. \end{aligned} \quad (13)$$

Thus, assuming  $R_{J|Kl}=1$  and  $\Delta t \geq 0$ , upper and lower bounds on the elements of the Markov process  $\mathcal{W}$  given by Eq. (3) are determined as follows:

$$\begin{aligned} \rho_r \underline{F}_{K,l}^{(r)} \hat{S}_{I,J}^{(r)} \exp(-\Delta t \tilde{D}_{Kl}) &\leq \hat{W}_{I,J}^{(r)} \exp(-\Delta t D_{JJ}) \\ &\leq \rho_r \tilde{F}_{K,l}^{(r)} \hat{S}_{I,J}^{(r)} \exp(-\Delta t \underline{D}_{Kl}). \end{aligned} \quad (14)$$

These desired bounds on reaction probability rates  $\hat{W}_{I,J}^{(r)} \exp(-\Delta t D_{JJ})$  follow from the simple bounds of Eq. (10) on  $n'_a$  as a function of  $n_a$  and  $l$ .

## D. Exploitation of probability bounds

We now use the bounds of Eq. (14) to derive the key update equations of the ER-leap algorithm. The resulting ER-leap algorithm will be assembled from these equations and discussed in Sec. II E, followed by computational experiments in Sec. III. In this section we perform the required calculations to derive the key update equations.

### 1. Rejection sampling

Rejection sampling<sup>16</sup> allows one to exploit probability bounds in exact sampling, as follows: given a target distribution  $P(x)$  and an algorithm for sampling from a related distribution  $P'(x)$  and from the uniform distribution  $U(u)$  on  $[0,1]$  and if

$$P(x) < MP'(x)$$

for some constant  $M > 1$ , then  $P(x)$  satisfies

$$P(x) = P'(x) \frac{P(x)}{MP'(x)} + (1 - 1/M)P(x),$$

and therefore also

$$\begin{aligned} P(x) = \int P'(x') dx' \int U(u) du \left[ \mathbf{1}\left(u < \frac{P(x')}{MP'(x')}\right) \right. \\ \left. \cdot \delta(x - x') + \mathbf{1}\left(u \geq \frac{P(x')}{MP'(x')}\right) \cdot P(x) \right], \end{aligned} \quad (15)$$

which constitutes a mixture distribution, that can be applied recursively as needed to sample from  $P(x)$ . Pseudocode for sampling  $P(x)$  according to Eq. (15) is as follows (where “//” introduces a comment):

```
while not accepted {
  sample  $P'(x)$  and  $U(u)$ ; //  $P'(x)$  only approximates  $P(x)$ 
  compute  $\text{Accept}(x) = P(x)/(MP'(x))$  // acceptance probability;
  if  $u < \text{Accept}(x)$  then accept  $x$ ;
} // now  $P(x)$  is sampled exactly
```

What is essential in applying this algorithm is to find a provable strict upper bound  $\tilde{P}(x) = MP'(x)$  for  $P(x)$  (where  $M > 1$ ), which is not a probability distribution but which when normalized yields a probability distribution  $P'(x)$  that is easier to sample than  $P(x)$ . We also want acceptance to be likely for computational efficiency; for that reason  $M$  should be as close to 1 as possible, so that the bound on  $P(x)$  is as tight as possible for a given computational cost.

But what if  $P(x)$  is expensive to compute? Then  $\text{Accept}(x)$  will also be expensive to compute and rejection sampling may be prohibitively expensive, even for a good approximating  $P'(x)$ . A solution to this problem is possible if a cheap lower bound for  $P(x)$  is available. Suppose there is a function  $\underline{A}(x)$  such that

$$0 \leq \underline{A}(x) \leq \text{Accept}(x) \equiv P(x)/(MP'(x)) < 1. \quad (16)$$

Then

$$\text{Accept}(x) = \underline{A}(x) \cdot 1 + (1 - \underline{A}(x)) \cdot Q(x),$$

where



$$Q(x) \equiv \left( \frac{\text{Accept}(x) - \underline{A}(x)}{1 - \underline{A}(x)} \right),$$

and  $\text{Accept}(x)$  becomes a mixture of probabilities defined over the pair of actions (accept, reject). Then we have the following “accelerated rejection sampling algorithm,” in pseudocode:

```

while not accepted {
  sample  $P'(x)$  and  $U(u)$ ; // cheap but approximate
  compute  $\underline{A}(x)$ ; // cheap
  if  $u < \underline{A}(x)$  then accept  $x$ ;
  else {
    compute  $\text{Accept}(x) = P(x)/MP'(x)$ ; // expensive
    compute  $Q(x) = (\text{Accept}(x) - \underline{A}(x)) / (1 - \underline{A}(x))$ 
    //  $\underline{A}(x) < 1 \Rightarrow 1 - \underline{A}(x) \neq 0$ 
    sample  $U(u)$ ;
    if  $u < Q(x)$  then accept  $x$ ;
    else reject  $x$ ;
  }
}

```

Again, the bound  $\underline{A}(x) \leq \text{Accept}(x)$  should be as tight as possible for a given level of computational cost, to maximize the probability of early and therefore low-cost acceptance. A natural measure of the tightness of this bound is  $\int \underline{A}(x) dx \leq 1$ , which should be as close to 1 as possible given cost considerations. However, even if  $\underline{A}(x) = 0$  for some values of  $x$ , the algorithm still samples the distribution  $P(x)$  exactly.

We now seek  $M$ ,  $P'(x)$ , and  $\underline{A}(x)$  for a run of  $L$  successive reaction events in the SSA algorithm.

## 2. Equivalent Markov process

In this section we will use algebraic manipulations to transform the formula for SSA [Eq. (8)] into an equivalent form [Eq. (18)] that represents an accelerated rejection sampling algorithm, as outlined in Sec. II D 1.

The first step in the algebraic derivation is to identify a probability distribution equivalent to  $L$  steps of the original SSA Markov process, which can itself be iterated to create a new, equivalent Markov process. The target distribution  $P$  is [from Eq. (8)]

$$[\hat{W} \exp(-\Delta t D)]^L \circ \text{Pr}(\cdot | K, 0).$$

From Eq. (14),

$$\begin{aligned} \hat{W}_{I,J} \exp(-t_k D_{JJ}) &= \left( \sum_r \rho_r \hat{S}_{I,J}^{(r)} \left( \frac{F_I^{(r)}}{\tilde{F}_{K,l-1}^{(r)}} \right) \tilde{F}_{K,l-1}^{(r)} \right) \\ &\quad \times \exp(-t_k (D_{JJ} - \underline{D}_{kl})) \exp(-t_k \underline{D}_{kl}). \end{aligned}$$

Expand out the ordered matrix product for states  $J$  reachable from  $K$  after  $L$  steps

$$\begin{aligned} R_{J|KL} = 1 &\Rightarrow \left[ \prod_{k=L-1 \searrow 0} \hat{W} \exp(-\tau_k D) \right]_{I_L, I_0} \\ &= \sum_{\{I_k | k=1 \cdots L-1\}} \left[ \prod_{k=L-1 \searrow 0} \hat{W}_{I_{k+1}, I_k} \exp(-\tau_k D_{I_k, I_k}) \right] \\ &= \sum_{\{I_k | k=1 \cdots L-1\}} \sum_{\{r_k\}} \prod_{k=L-1 \searrow 0} \left[ \left( \rho_{r_k} \hat{S}_{I_{k+1}, I_k}^{(r_k)} \left( \frac{F_{I_k}^{(r_k)}}{\tilde{F}_{I_0, L-1}^{(r_k)}} \right) \tilde{F}_{I_0, L-1}^{(r_k)} \right) \right. \end{aligned}$$

$$\begin{aligned} &\times \exp(-\tau_k (D_{I_k, I_k} - \underline{D}_{I_0, L-1})) \exp(-\tau_k \underline{D}_{I_0, L-1}) \\ &= \sum_{\{r_k | k=1 \cdots L-1\}} \sum_{\{I_k\}} \left[ \prod_{k=L-1 \searrow 0} \hat{S}_{I_{k+1}, I_k}^{(r_k)} \right] \left[ \prod_{k=L-1 \searrow 0} \rho_{r_k} \tilde{F}_{I_0, L-1}^{(r_k)} \right] \\ &\times \left[ \prod_{k=L-1 \searrow 0} \left( \frac{F_{I_k}^{(r_k)}}{\tilde{F}_{I_0, L-1}^{(r_k)}} \right) \exp(-\tau_k (D_{I_k, I_k} \right. \\ &\quad \left. - \underline{D}_{I_0, L-1})) \exp\left(-\left(\sum_k \tau_k\right) \underline{D}_{I_0, L-1}\right) \right]. \end{aligned}$$

Now  $\sum_r \hat{S}_{I,J}^{(r)} = 1$  allows a change in representation to eliminate the inner state sums,

$$I_k = I_k(r_{k-1}, I_{k-1}) = \hat{I}_k(\mathbf{r} = [r_0, \dots, r_l], I_0),$$

$$\begin{aligned} &\left[ \prod_{k=L-1 \searrow 0} \hat{W} \exp(-\tau_k D) \right]_{I_l, I_0} \\ &= \sum_{\{r_k | k=1 \cdots L-1\}} \left[ \prod_{k=L-1 \searrow 0} \rho_{r_k} \tilde{F}_{I_0, L-1}^{(r_k)} \right] \exp\left(-\left(\sum_k \tau_k\right) \underline{D}_{I_0, L-1}\right) \\ &\times \left[ \prod_{k=L-1 \searrow 0} \left( \left( \frac{F_{I_k(r, I_0)}^{(r_k)}}{\tilde{F}_{I_0, L-1}^{(r_k)}} \right) \exp(-\tau_k (D_{I_k(r, I_0), I_k(r, I_0)} \right. \right. \\ &\quad \left. \left. - \underline{D}_{I_0, L-1})) \right) \right]. \end{aligned}$$

Define new rule probabilities,

$$p_{r|K,l} = \rho_r \tilde{F}_{K,l}^{(r)} \tilde{D}_{Kl} \equiv \frac{\rho_r \tilde{F}_{K,l}^{(r)}}{\sum_r \rho_r \tilde{F}_{K,l}^{(r)}}. \quad (17)$$

Then,

$$\begin{aligned} &\left[ \prod_{k=L-1 \searrow 0} \hat{W} \exp(-\tau_k D) \right]_{I_l, I_0} \\ &= \sum_{\{r_k | k=1 \cdots L-1\}} \left[ \prod_{k=L-1 \searrow 0} p_{r_k | I_0, L-1} \right] (\tilde{D}_{I_0, L-1})^l \\ &\times \exp\left(-\left(\sum_k \tau_k\right) \underline{D}_{I_0, L-1}\right) \left[ \prod_{k=L-1 \searrow 0} \left( \left( \frac{F_{I_k(r, I_0)}^{(r_k)}}{\tilde{F}_{I_0, L-1}^{(r_k)}} \right) \right. \right. \\ &\quad \left. \left. \times \exp(-\tau_k (D_{I_k(r, I_0), I_k(r, I_0)} - \underline{D}_{I_0, L-1})) \right) \right] \\ &= \sum_{\{r_k | k=1 \cdots L-1\}} e_1(\mathbf{r}) e_2(\mathbf{r}), \end{aligned}$$

where

$$e_1(\mathbf{r}) \equiv \left[ \prod_{k=L-1 \searrow 0} p_{r_k | I_0, L-1} \right] (\tilde{D}_{I_0, L-1})^l \exp\left(-\left(\sum_k \tau_k\right) \underline{D}_{I_0, L-1}\right),$$

$$e_2(\mathbf{r}) \equiv \left[ \prod_{k=L-1 \searrow 0} \left( \left( \frac{F_{I_k(\mathbf{r}, I_0)}^{(r_k)}}{\tilde{F}_{I_0, L-1}^{(r_k)}} \right) \times \exp(-\tau_k(D_{I_k(\mathbf{r}, I_0), I_k(\mathbf{r}, I_0)} - D_{I_0, L-1})) \right) \right].$$

We define an arbitrary ordering “ $\leq$ ” on the reaction types or channels indexed by  $r$ , so the reactions events are “sorted” by type if and only if  $r_0 \leq r_1 \leq \dots \leq r_{L-1}$ . Let  $\sigma$  denote a permutation on  $L$  elements which we may apply to this ordering to get an unordered sequence of rules  $\mathbf{r} = \{r_k | k = 0 \dots L-1\}$ . For a given unordered  $\mathbf{r}$  we further restrict the permutations  $\sigma$  to be those which do not interchange equal  $r$ 's; this will avoid double counting.

Then in the foregoing expression  $\sum_{\{r_k | k=1 \dots L-1\}} e_1(\mathbf{r}) e_2(\mathbf{r})$  we may replace the multiple sum over reactions with a sum over permutations  $\sigma$  that order the reactions, and an outer sum over the possible *ordered* reaction sets,

$$\begin{aligned} & \sum_{\{r_k | k=1 \dots L-1\}} e(\mathbf{r}) \\ &= \sum_{\{r_0 \leq \dots \leq r_{L-1}\}} \sum_{\{\sigma | \sigma \text{ permutes unequal } r's\}} e_1(\sigma(\mathbf{r})) e_2(\sigma(\mathbf{r})). \end{aligned}$$

The number of  $r$ 's taking each possible value  $1 \dots R$  is denoted  $[s_1, \dots, s_R] = \mathbf{s}(\mathbf{r})$ ; these are the number of times each type of reaction occurs in the sequence  $\mathbf{r}$ . The components of  $\mathbf{s}$  and  $\mathbf{r}$  are therefore related as follows:

$$s_r = \sum_{k=0}^{L-1} \delta(r_k - r),$$

which satisfies

$$s_r \in \mathbb{N} \quad \text{and} \quad \sum_r s_r = L.$$

Also the ordered list of  $r$ 's is determined by the vector  $\mathbf{s}$ ,

$$r_k = \min \left\{ r | k \leq \sum_{i=1}^r s_i \right\}.$$

Hence we may replace the sum over ordered  $\mathbf{r}$  with a sum over constrained  $\mathbf{s}$ ,

$$\begin{aligned} & \sum_{\{r_k | k=1 \dots L-1\}} e(\mathbf{r}) \\ &= \sum_{\{s | s_r \in \mathbb{N}, \sum_r s_r = L\}} \sum_{\{\sigma | \sigma \text{ permutes unequal } r's\}} e_1(\sigma(\mathbf{r})) e_2(\sigma(\mathbf{r})), \end{aligned}$$

$e_1(\mathbf{r})$  however, depends on  $\mathbf{r}$  only through  $\mathbf{s}$ , which is permutation invariant,

$$e_1(\mathbf{r}) \equiv \tilde{e}_1(\mathbf{s}(\mathbf{r})) = \tilde{e}_1(\mathbf{s}(\sigma(\mathbf{r}))) = e_1(\sigma(\mathbf{r})).$$

Hence

$$\begin{aligned} & \sum_{\{r_k | k=1 \dots L-1\}} e_1(\sigma(\mathbf{r})) e_2(\sigma(\mathbf{r})) \\ &= \sum_{\{s | s_r \in \mathbb{N}, \sum_r s_r = L\}} \tilde{e}_1(\mathbf{s}(\mathbf{r})) \sum_{\{\sigma | \sigma \text{ permutes unequal } r's\}} e_2(\sigma(\mathbf{r})) \\ &= \sum_{\{s | s_r \in \mathbb{N}, \sum_r s_r = L\}} \tilde{e}_1(\mathbf{s}(\mathbf{r})) \left( \sum_{\{\sigma | \sigma \text{ permutes unequal } r's\}} e_2(\sigma(\mathbf{r})) \right) \\ &= \sum_{\{s | s_r \in \mathbb{N}, \sum_r s_r = L\}} \tilde{e}_1(\mathbf{s}(\mathbf{r})) \binom{L}{s_1 \dots s_R} \\ & \times \langle e_2(\sigma(\mathbf{r})) \rangle_{\{\sigma \text{ permutes unequal } r's\}}, \end{aligned}$$

where  $\langle \dots \rangle_S$  denotes averaging over the given set  $S$ . On the other hand,  $e_2(\mathbf{r})$  is invariant under any permutation  $\sigma$  which *only* exchanges equal  $r$ 's, so

$$\begin{aligned} & \langle e_2(\sigma(\mathbf{r})) \rangle_{\{\sigma \text{ permutes unequal } r's\}} \\ &= \langle e_2(\sigma(\mathbf{r})) \rangle_{\{\sigma \text{ permutes integers } 1 \dots L\}}, \end{aligned}$$

and we find

$$\begin{aligned} & \sum_{\{r_k | k=1 \dots L-1\}} e_1(\sigma(\mathbf{r})) e_2(\sigma(\mathbf{r})) = \sum_{\{s | s_r \in \mathbb{N}, \sum_r s_r = L\}} \binom{L}{s_1 \dots s_R} \tilde{e}_1(\mathbf{s}(\mathbf{r})) \\ & \times \langle e_2(\sigma(\mathbf{r})) \rangle_{\{\sigma \text{ permutes } r's\}}. \end{aligned}$$

Consequently,

$$\begin{aligned} & \left[ \prod_{k=L-1 \searrow 0} \hat{W} \exp(-\tau_k D) \right]_{I_L, I_0} \\ &= \sum_{\{s | s_r \in \mathbb{N}, \sum_r s_r = L\}} \binom{L}{s_1 \dots s_R} \left[ \prod_{r=1}^R (p_{r|I_0, L-1})^{s_r} \right] \\ & \times (\tilde{D}_{I_0, L-1})^l \exp\left(-\left(\sum_k \tau_k\right) \tilde{D}_{I_0, L-1}\right) \\ & \times \left\langle \left[ \prod_{k=L-1 \searrow 0} \left( \frac{F_{I_k(\sigma(\mathbf{r}), I_0)}^{(r_k)}}{\tilde{F}_{I_0, L-1}^{(r_k)}} \right) \right. \right. \\ & \left. \left. \times \exp(-\tau_k(D_{I_k(\sigma(\mathbf{r}), I_0), I_k(\sigma(\mathbf{r}), I_0)} - D_{I_0, L-1})) \right) \right] \right\rangle_{\{\sigma | \sigma\}}. \end{aligned}$$

This can be decomposed into more elementary probability distributions,

$$\begin{aligned} & \left[ \prod_{k=L-1 \searrow 0} \hat{W} \exp(-\tau_k D) \right]_{I_L, I_0} \\ &= \frac{(\tilde{D}_{I_0, L-1})^L}{(\tilde{D}_{I_0, L-1})^L} \sum_{\{s | s_r \in \mathbb{N}, \sum_r s_r = L\}} \text{Multinomial}(\mathbf{s} | \mathbf{p}, L) \\ & \times \text{Erlang}\left(\sum_k \tau_k | L, \tilde{D}_{I_0, L-1}\right) \text{UniformSimplex}(\boldsymbol{\tau}; L) \\ & \times \text{Accept}(\mathbf{s}, L, \boldsymbol{\tau}), \end{aligned} \tag{18}$$

where

$$\text{Multinomial}(s|\mathbf{p}, L) = \binom{L}{s_1 \dots s_R} \left[ \prod_{r=1}^R (p_r|_{I_0, L-1})^{s_r} \right],$$

with

$$p_r|_{I_0, L-1} = \frac{\rho_r \tilde{F}_{I_0, L-1}^{(r)}}{\sum_r \rho_r \tilde{F}_{I_0, L-1}^{(r)}}$$

$$\text{Erlang}(t; l, \lambda) \equiv \lambda^l e^{-\lambda t} t^{l-1} / (l-1)!,$$

$$\text{where } \langle t \rangle_{\text{Erlang}} = l/\lambda.$$

We note that the Erlang distribution is the Gamma distribution specialized to integer-valued shape parameter  $l$ .

Also

$$\text{UniformSimplex}(\boldsymbol{\tau}; L) = 1 / \left( \frac{L^{L-1}}{(L-1)!} \right),$$

and the acceptance probability

$$\text{Accept}(s, l, \boldsymbol{\tau}) \equiv \langle P_\sigma \rangle_{\{\sigma|s\}},$$

where

$$P_\sigma = \left[ \prod_{k=L-1 \searrow 0} \left( \frac{F_{I_k(\sigma(r), I_0)}^{(r_k)}}{\tilde{F}_{I_0, L-1}^{(r_k)}} \right) \right] \times \exp \left( - \sum_k \tau_k (D_{I_k(\sigma(r), I_0), I_k(\sigma(r), I_0)} - D_{I_0, L-1}) \right). \quad (19)$$

From the definition of  $P_\sigma$  in Eq. (19) and the fact that  $\tilde{F}$  and  $\underline{D}$  are bounds, it follows that  $\text{Accept}(s, l, \boldsymbol{\tau}) \leq 1$ . Also, if  $R_{J|KL-1}=0$  (so that state  $J$  is not reachable from state  $K$  after  $L-1$  steps of SSA) then  $P_\sigma=0$ , so that Eq. (18) still agrees with Eq. (8) despite the restriction to  $R_{J|KL-1}=1$  stated in the foregoing calculation.

Thus, Eq. (18) provides an equivalent probability distribution and Markov process to Eq. (8).

### 3. Efficient rejection sampling algorithm

We now seek  $M$  and  $P'$  and  $\underline{A}(x)$  among the factors of Eq. (18). We can upper-bound and lower-bound  $P_\sigma$  of Eq. (19),

$$\underline{P} \left( s, \sum_k \tau_k, L \right) \leq P_\sigma \leq 1, \quad (20)$$

where

$$\underline{P} \left( s, \sum_k \tau_k, L \right) \equiv \left[ \prod_{r=1}^R \left( \frac{F_{I_0, L-1}^{(r)}}{\tilde{F}_{I_0, L-1}^{(r)}} \right)^{s_r} \right] \exp \left( - \left( \sum_k \tau_k \right) \times (\tilde{D}_{I_0, L-1} - D_{I_0, L-1}) \right). \quad (21)$$

Note that  $\underline{P}$  does not depend on  $\sigma$ . This allows us to use rejection sampling<sup>16</sup> to transform samples of the bounding distribution,

$$g(s, \boldsymbol{\tau}) = \text{Multinomial}(s|\mathbf{p}, L)$$

$$\text{Erlang} \left( \sum_k \tau_k | L, D_{I_0, L-1} \right)$$

$$\text{UniformSimplex} \left( \boldsymbol{\tau}; l, \sum_{k=0}^{L-1} \tau_k \right)$$

into samples of the target distribution,

$$f(s, \boldsymbol{\tau}) = f(s, \boldsymbol{\tau}) \frac{(\tilde{D}_{I_0})^L}{(\underline{D}_{I_0})^L} \text{Accept}(s, L, \boldsymbol{\tau})$$

since the ratio  $f(s, \boldsymbol{\tau})/g(s, \boldsymbol{\tau})$  is bounded above by  $M = (\tilde{D}_{I_0, L-1}/\underline{D}_{I_0, L-1})^L \geq 1$ .  $g(s, \boldsymbol{\tau})$  plays the role of  $P'(x)$  in the rejection sampling algorithm of Sec. II D 1,  $f(s, \boldsymbol{\tau})$  plays the role of  $P(x)$ , and  $M$  has just been defined. This bound is independent of all randomly chosen variables  $s, t, \boldsymbol{\tau}, \sigma$  and just restores the probability otherwise lost in rejection sampling due to the  $\text{Accept}(s, L, \boldsymbol{\tau})$  factor being  $\leq 1$ . It remains to define  $\underline{A}(x)$  for the “efficient rejection sampling” algorithm.

In order to apply the efficient rejection sampling algorithm of Sec. II D 1, we need to find a lower bound  $\underline{A}(x)$  for  $\text{Accept}(s, l, \boldsymbol{\tau}) = \langle P_\sigma \rangle_{\{\sigma|s\}}$ . Fortunately  $P(s, \Sigma_k, \tau_k, L)$  is a lower bound for  $P_\sigma$ , so we can just average over  $\sigma$  compatible with  $s$ . Then  $P_\sigma$  may be expressed as a mixture distribution,

$$P_\sigma = \underline{P} \cdot 1 + (1 - \underline{P}) \cdot Q_\sigma,$$

where

$$Q_\sigma = \left( \frac{P_\sigma - \underline{P}}{1 - \underline{P}} \right) \leq 1, \quad (22)$$

and thus

$$\langle P_\sigma \rangle_{\{\sigma|s\}} = \underline{P} \cdot 1 + (1 - \underline{P}) \cdot \langle Q_\sigma \rangle_{\{\sigma|s\}}.$$

However, instead of numerically averaging over  $\sigma$  to compute  $\langle Q_\sigma \rangle_{\{\sigma|s\}}$  in each iteration, we will instead draw a single sample of  $\sigma$  and use that sample's value of  $Q_\sigma$ . This step is also exact since we can just define  $\text{Accept}(\boldsymbol{\sigma}, L, \boldsymbol{\tau}) = \text{Accept}(s, L, \boldsymbol{\tau}) \cdot \text{Pr}(\boldsymbol{\sigma}|s)$ , where  $\text{Pr}(\boldsymbol{\sigma}|s)$  is uniform, and apply accelerated rejection sampling to  $f(s, \boldsymbol{\tau}) \text{Pr}(\boldsymbol{\sigma}|s)$  using the corresponding bounds  $f(s, \boldsymbol{\tau}) \text{Pr}(\boldsymbol{\sigma}|s)$  for  $P_\sigma$  for  $\underline{A}(x)$ .

Algorithmically this expression can be sampled from as follows. First compute  $\underline{P}$ . Then with probability  $\underline{P}$ , accept the “current” candidate move determined by all the other distributions. In the relatively unlikely event (probability  $1 - \underline{P}$ ) that the move is not immediately accepted this way, we then draw a random  $\sigma$  given  $s$  and compute its  $Q_\sigma$ . Then, accept the current move with probability  $Q_\sigma$ , and with probability



$1 - Q_\sigma$  reject the current move, draw a new one, and iterate. For computational efficiency the initial acceptance rate  $\underline{P}$  should be high. Pseudocode for the resulting algorithm will be presented in Sec. II E.

## E. Exact R-leap algorithm

We now assemble the ER-leap algorithm from the key update equations derived in previous sections: Equations (11), (13), (17), (18), (21), (19), and (22).

### 1. Algorithm summary

We adapt the efficient rejection sampling algorithm of Sec. II D 1, with the random variables  $s$ ,  $\sigma$ , and  $\tau$ , and the expressions for  $P$ ,  $P'$ ,  $M$ , and  $\underline{A}$  of Sec. II D 3, into pseudocode for the core of the resulting exact R-leap algorithm:

```

set counters  $n$ ,  $\sum_k P_k$ ,  $\sum_k P_k^2$  to zero
starting at state  $I_0$ , initial time  $t_0$ , and user-specified
initial leap  $L$ 
while  $t \leq T$  {
  if  $L$  equals 1 then perform one SSA step,
    set  $\underline{P}=1$  (for dynamic  $L$  update counter);
  else repeat {
    compute or update the bounds on  $F$ 's,  $D$ 's for  $I_0$ ,
      by Equation (11) and (13);
    compute  $\mathbf{p}$ :  $p_{r|I_0,l-1} = p_r \tilde{F}_{I_0,l-1}^{(r)} / \tilde{D}_{I_0,l}$ ;
    sample  $s$  from Multinomial ( $s|\mathbf{p}, l$ )
      (using sorted sequential Binomials,
      for efficiency, as in R-leap);
    sample  $\sum_k \tau_k$  from Erlang ( $\sum_k \tau_k | L, \underline{D}_{I_0,l}$ );
    compute  $\underline{P}(s, \sum_k \tau_k, L)$  by Equation (21);
    //cheap
    with probability  $\underline{P}$  {
      accept step;
    } otherwise {
      // expensive
      sample  $\sigma$  from permutations consistent with  $s$ 
      compute  $P_\sigma \in [\underline{P}, 1]$  by Equation (19);
      compute  $Q_\sigma = \left( \frac{P_\sigma - \underline{P}}{1 - \underline{P}} \right)$ ;
      with probability  $Q_\sigma$  accept step otherwise reject
      step;
    }
  } until step accepted;
  update  $I_0$ ;
  increment  $n$ ,  $\sum_k P_k = \sum_k P_k + \underline{P}$ ,  $\sum_k P_k^2 = \sum_k P_k^2 + \underline{P}^2$ ;
  if  $n \geq b$  then update  $L$  according to Equation (25).
  if  $L$  changed or Uniform  $\in [0, 1]$ 
    is below  $1/L^2$ 
    then set counters  $n$ ,  $\sum_k P_k$ ,  $\sum_k P_k^2$  to zero;
} until done

```

The implementation used in this paper is written in C++ and contains around 600 lines of code for the core components.

## 2. Acceptance ratio analysis

A preliminary analysis looks very permissive of large  $L$ ,

$$\underline{\Delta}_a \equiv \min_r \Delta m_a^r, \quad \tilde{m}_a \equiv \max_r m_a^r, \quad (23)$$

$$\tilde{\Delta}_a \equiv \max_r \Delta m_a^r, \quad \tilde{m} \equiv \max_r \sum_a m_a^r.$$

Then for large  $n_a$ , such that

$$n_a \gg (L-1)|\underline{\Delta}_a| + \tilde{m}_a,$$

we further insist that

$$L(L-1) \leq \frac{\min_a n_a}{\tilde{m} \max_a (\tilde{\Delta}_a - \underline{\Delta}_a + \tilde{m}_a)} \log(1/\alpha),$$

where  $\alpha \in [0, 1]$  is the minimal early-acceptance rate (should be close to 1 for efficiency). If  $\alpha = 1 - \epsilon$ , this becomes roughly

$$L \leq \sqrt{\frac{\epsilon \min_a n_a}{\tilde{m} \max_a (\tilde{\Delta}_a - \underline{\Delta}_a + \tilde{m}_a)}}.$$

## 3. Asymptotic cost of update

The asymptotic computational cost of simulating with ER-leap can be analyzed. The amount of computation required to calculate and sample  $\underline{P}$  is dominated by the time required to calculate the reaction probability rates or propensities. The asymptotic cost of this will be  $O(R)$ , where  $R$  is the number of reaction types or channels. In the event that an “early” sample is rejected, the more thorough sampling and calculation of  $P_\sigma$ , that becomes necessary, will be dominated by the recalculation of the reaction probability rates for each of the  $L$  reaction events. Therefore, computing  $P_\sigma$  will have asymptotic cost  $O(LR)$ . Thus, during simulation the expected computation per attempted leap will be the inevitable cost of calculating  $\underline{P}$  plus the cost of calculating  $P_\sigma$ , which occurs with probability  $(1 - \langle \underline{P} \rangle)$ . So the computational cost for one leap attempt can be estimated as

$$O(R + (1 - \langle \underline{P} \rangle)LR). \quad (24)$$

To calculate the expected CPU cost per reaction event, we assume that all  $P_\sigma$  samples are rejected. This yields a lower bound on the expected number of accepted reaction events per leap, which will be  $\langle \underline{P} \rangle L$ . Additionally, the cost for one SSA step will be  $O(R)$  and the number of reactions events per step will be 1. Thus the per-event costs for ER-leap and SSA will be

$$\text{ERleap cost} = \frac{\text{ERleap leap cost}}{\text{reaction events}} \leq \frac{R + (1 - \langle \underline{P} \rangle)LR}{\langle \underline{P} \rangle L},$$

$$\text{SSA cost} = \frac{\text{SSA step cost}}{\text{reaction events}} = \frac{R}{1}.$$

The cost ratio between SSA and ER-leap is therefore

$$\text{cost ratio} = \frac{\text{ERleap cost}}{\text{SSA cost}} \leq \frac{1 + (1 - \langle \underline{P} \rangle)L}{\langle \underline{P} \rangle L}.$$

When this cost ratio is less than 1, ER-leap will be asymptotically faster than SSA. This is the case whenever  $\langle P \rangle > (1+L)/2L$  which in turn is  $>1/2$ . Finally, taking the inverse of the cost ratio gives us the lower bound on the speedup of ER-leap over SSA, which is

$$\text{speedup} \propto \frac{\langle P \rangle L}{1 + (1 - \langle P \rangle)L}.$$

The required data structures and space requirements for ER-leap do not go significantly beyond what is conventional for SSA simulation: Each reaction needs a list of input/output species, so an array is used to remember the state of the system as well as a temporary state copy when calculating  $P_\sigma$ , and arrays are used to store  $\sigma$ ,  $\tau$ , and the maximal and minimal  $\tilde{\Delta}_a$  and  $\underline{\Delta}_a$  values.

#### 4. Dynamic choice of $L$

ER-leap efficiency depends on finding an  $L$  which optimally balances the benefits of having a large  $L$  versus the potential inefficiencies that would result from sample rejections. Our heuristic is described here.

Recall from Eq. (24) that the cost of calculating early-acceptance samples will be  $O(R)$  and the expected cost of calculating the late acceptance samples is  $O((1 - \langle P \rangle)L R)$  for each leap attempt. Balancing these costs yields  $L = 1/(1 - \langle P \rangle)$  or  $\langle P \rangle = (L-1)/L$ . So, during simulation the goal is to choose an  $L$  satisfying  $\langle P \rangle \approx (L-1)/L$ . This is done by sampling  $P$  to obtain an estimate of the “true” value of  $\langle P \rangle$  (for which we take at least  $b=5$  samples). Then  $L$  is increased or decreased by at most 1, to minimize the error in the condition  $\langle P \rangle \approx (L-1)/L$ , where the  $\beta$  parameter is introduced to tune differences in CPU running time between the  $P$  and  $P_\sigma$  calculations. Experiments (not presented) show good performance when  $\beta=2/3$  and this is used in all subsequent experiments.

Confidence intervals for our estimate of  $\mu$ , the mean of  $P$ , come from the central limit theorem,

$$\mu = \bar{\mu} \pm z \sqrt{\frac{\sigma^2}{n}} = \bar{\mu} \pm E_{\text{rror}},$$

where statistics for calculating the sample mean and sample variance ( $\bar{\mu}, \sigma^2$ ) are gathered from  $P$  during simulation,  $z$  is a “confidence factor” (we used  $z=1.7$  in experiments), and  $n$  is the number of samples. Given the goal  $\langle P \rangle$  for a given  $L$ , namely  $h(L) = ((L-1)/L)^{1/\beta}$ , the rule for updating  $L$  to a new  $L'$  is

$$L' = \begin{cases} L+1, & \text{if } h(L) < \bar{\mu} - E_{\text{rror}} \text{ and } h(L+1) < \bar{\mu} + E_{\text{rror}} \\ L-1, & \text{if } \bar{\mu} - E_{\text{rror}} < h(L-1) \text{ and } \bar{\mu} + E_{\text{rror}} < h(L) \\ L, & \text{otherwise,} \end{cases} \quad (25)$$

which changes  $L$  whenever the interval  $\{\bar{\mu} - E_{\text{rror}}, \bar{\mu} + E_{\text{rror}}\}$  does not contain  $h(L)$ , and changing  $L$  by one would either (a) put  $h(L')$  within this interval or (b) put  $h(L')$  in between

$h(L)$  and this interval, thereby bringing it closer to the desired interval.

Finally, to avoid getting “stuck” on a particular  $L$ , the counters are occasionally reset with probability  $1/L^2$ .

#### 5. An illustrative example

As a specific example of the use of the ER-leap algorithm, consider the two-reaction dimerization process  $\{2S_1 \xrightleftharpoons[\rho_2]{\rho_1} S_2\}$  with forward and reverse reactions  $r=1$  and  $r=2$ .

Recall from Eq. (9) that the instantaneous rates of firing, also called propensities, for each reaction are given by

$$a_1(\mathbf{n}) = \rho_1 n_1 (n_1 - 1), \quad a_2(\mathbf{n}) = \rho_2 n_2.$$

[Some authors divide  $a_1(\mathbf{n})$  by 2 to “avoid double counting,” but our convention is to absorb this factor of 2 into  $\rho_1$  and thereby remain notationally consistent with the law of mass action.) ER-leap requires upper and lower bounds on the propensities for each reaction at any of  $L$  reaction event “steps.” The bounds are not required to be tight, but here it is easy to find the tightest bounds using Eq. (11),

$$\tilde{a}_1(\mathbf{n}) = \rho_1 (n_1 + 2(L-1))((n_1 + 2(L-1) - 1)),$$

$$\underline{a}_1(\mathbf{n}) = \rho_1 (n_1 - 2(L-1))((n_1 - 2(L-1) - 1)),$$

$$\tilde{a}_2(\mathbf{n}) = \rho_2 (n_2 + (L-1)),$$

$$\underline{a}_2(\mathbf{n}) = \rho_2 (n_2 - (L-1)).$$

The upper bound  $\tilde{a}_1$  comes from the extreme situation in which all  $L$  reactions are of type  $r=2$ . Two  $S_1$  are produced every time  $r=2$  fires. So we calculate the upper bounding propensities with an upper bound for  $S_1$ :  $\tilde{n}_1 = n_1 + 2(L-1)$ . Recall that  $(L-1)$  is used instead of  $L$  because about the bounds apply *just before* the  $L$ th step occurs. The other bounds are calculated in the same way.

Given bounds on  $a_1$  and  $a_2$ , we can sample the reactions and time step. First, the number of times  $r=1$  and  $r=2$  are fired  $(s_1, s_2)$  is sampled from a multinomial distribution (here equivalent to a binomial) with parameters  $((\tilde{a}_1(\mathbf{n})/\tilde{a}_0(\mathbf{n}), \tilde{a}_2(\mathbf{n})/\tilde{a}_0(\mathbf{n})), L)$ , where  $\tilde{a}_0(\mathbf{n}) = \tilde{a}_1(\mathbf{n}) + \tilde{a}_2(\mathbf{n})$ . Next, the total time step  $\tau$  is sampled from the Erlang (Gamma with an integer second argument) distribution with parameters  $(q_0(\mathbf{n}), L)$ .

To compute the probability of early acceptance, Eq. (21) is used. This simplifies to

$$\begin{aligned} \text{Prob}_{\text{early}}(\mathbf{s}, \tau) &= \left( \frac{F_{I_0, L-1}^{(1)}}{\tilde{F}_{I_0, L-1}^{(1)}} \right)^{s_1} \left( \frac{F_{I_0, L-1}^{(2)}}{\tilde{F}_{I_0, L-1}^{(2)}} \right)^{s_2} \exp(-(\tau_1 + \tau_2)) \\ &\quad \times (\tilde{D}_{I_0, L-1} - D_{I_0, L-1}) \\ &= \left( \frac{q_1(\mathbf{n})}{\tilde{a}_1(\mathbf{n})} \right)^{s_1} \left( \frac{q_2(\mathbf{n})}{\tilde{a}_2(\mathbf{n})} \right)^{s_2} \exp(-\tau(\tilde{a}_0(\mathbf{n}) - q_0(\mathbf{n}))). \end{aligned}$$

We accept the sample  $(\mathbf{s}, \tau)$  *early*, and with little computational cost, with  $\text{Prob}_{\text{early}}$ . If there is no early acceptance, the probability of late acceptance must be calculated. To calculate this first we must sample an *ordering* of reactions,  $\sigma$ .

This ordering is just a random shuffling of the  $L$  reactions. So our sample may look like  $\sigma = \{r=1, r=1, r=2, \dots, r=1\}$ . Next, we need to sample the length of individual time steps for each reaction,  $\{\tau_1, \tau_2, \dots, \tau_L\}$ . This can be done by independently sampling  $L$  unit exponential random variables and “normalizing” them so their sum is  $\tau$ . It is now possible to calculate the true probability of acceptance from Eq. (19),

$$\begin{aligned} \text{Prob}_{\text{accept}}(\sigma, \{\tau_i\}) &= \left( \frac{1}{\tilde{F}_{I_0, L-1}^{(1)}} \right)^{s_1} \left( \frac{1}{\tilde{F}_{I_0, L-1}^{(2)}} \right)^{s_2} \prod_{i=1}^L F_{I_i, L-1}^{(\sigma_i)} \\ &\quad \times \exp(-\tau_i(D_{I_i, L-1} - D_{I_0, L-1})) \\ &= \left( \frac{1}{\tilde{a}_1(\mathbf{n})} \right)^{s_1} \left( \frac{1}{\tilde{a}_2(\mathbf{n})} \right)^{s_2} \prod_{i=1}^L a_{\sigma_i}(\mathbf{n}_i) \\ &\quad \times \exp(-\tau_i(a_0(\mathbf{n}_i) - a_0(\mathbf{n}))). \end{aligned}$$

Here  $\tilde{a}(\mathbf{n})$  and  $a_0(\mathbf{n})$  are held constant during the calculation, but the true propensities  $a_{\sigma_i}(\mathbf{n}_i)$  are recalculated after each reaction  $\sigma_i$  occurs. State  $I_0$  corresponds to state vector  $\mathbf{n}$ , and  $I_i$  corresponds to  $\mathbf{n}_i$ , where  $i \in \{1 \dots L\}$  indexes the step number. With probability  $(\text{Prob}_{\text{accept}} - \text{Prob}_{\text{early}}) / (1 - \text{Prob}_{\text{early}})$  we accept the sample and update  $\mathbf{n}$ . Otherwise the sample is rejected.

In general, calculating the propensity bounds with Eqs. (11) and (13) can be made efficient by noting that the maximum and minimum amounts by which a species may change in one reaction event remain constant throughout the simulation. These  $\tilde{\Delta}_a$  and  $\underline{\Delta}_a$  values [defined in Eq. (23)] are calculated prior to simulation, and the bounding  $\tilde{n}_a$  is calculated as  $\tilde{n}_a = n_a + (L-1)\tilde{\Delta}_a$ , from Eq. (10). Then the propensity upper and lower bounds are calculated as conventional propensities except that the bounding  $\tilde{n}_a$  and  $\underline{n}_a$  are used for each reactant instead of  $n_a$ .

### III. NUMERICAL SIMULATIONS

The foregoing stochastic algorithms are implemented in the C++ programming language and run on a MacBook running OS X v10.5 with an Intel dual-core 1.83 GHz processor and 2.0 Gbytes of RAM. Experiments are performed with emphasis on exploring accuracy and speedup. We compare the present algorithm with the software developed for the  $\tau$ -leap and R-leap algorithms as reported in the R-leap paper.<sup>11</sup>

#### A. Accuracy

Here we verify ER-leap equivalence to SSA via numerical experiments. As an example of the tests performed in the CaliBayes test suite,<sup>17</sup> we consider the Galton–Watson stochastic process where analytic solutions for the mean and standard deviation are known. Mass-action stochastic kinetics are assumed. The solutions are compared to trajectories of many runs of SSA, ER-leap,  $\tau$ -leap, and R-leap.

Algorithm accuracy was validated using a statistical test as performed in CaliBayes. The  $i$ th sample at time  $t$  will be denoted  $X_t^{(i)}$  and is drawn from the random variable  $X^i$ . The analytic mean and standard deviation at time  $t$  are  $\mu_t$  and  $\sigma_t$ .

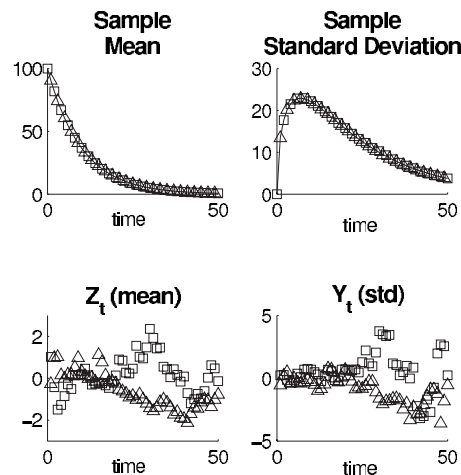


FIG. 1. ER-leap ( $\square$ ) with  $L=4$  and SSA ( $\triangle$ ) compared with the analytical (—) mean and standard deviation. Y-axis in units of molecules. The  $Z_t$  and  $Y_t$  values will be normally distributed, assuming SSA equivalence. Therefore values in the range  $(-3, 3)$  are considered reasonable. Galton–Watson stochastic process  $\{X \rightarrow 2X, X \rightarrow \emptyset\}$  with rate parameters  $\{1.0, 1.1\}$ , respectively, and  $X(0)=100$ . Simulation time is 50 s. Results from 20 000 runs.

Additionally,  $\bar{X}_t$  is the sample mean and  $\bar{S}_t$  is the sample standard deviation assuming  $E[X_t] = \mu_t$ . Using the central limit theorem, we eventually arrive to

$$Z_t = \sqrt{n} \frac{\bar{X}_t - \mu_t}{\sigma_t}, \quad Y_t = \sqrt{\frac{n}{2}} \left( \frac{\bar{S}_t^2}{\sigma_t^2} - 1 \right).$$

Under the null hypothesis that the simulator is correct, the  $Z_t$  and  $Y_t$  values should have a standard normal distribution. So most  $Z_t$  values are expected to lie in the range  $(-3, 3)$ . We further relax this constraint for  $Y_t$  to lie in the range  $(-5, 5)$  because the standard deviation is less likely to be normally distributed.

We performed this analysis on SSA and ER-leap. As Fig. 1 indicates,  $Z_t$  and  $Y_t$  are within the expected range for both simulation algorithms. This supports the notion that SSA and ER-leap draw from the same distribution.

To demonstrate the sensitivity of this test we also compute  $Z_t$  and  $Y_t$  for the approximate algorithms. Interestingly, all algorithms do not show strong errors in  $Y_t$ . However, the absolute values of  $Z_t$  for R-leap and  $\tau$ -leap are mostly greater than 3 (Fig. 2). This test indicates that SSA and ER-leap are equivalent with high certainty and it was sensitive enough to discover the error resulting from the assumptions made by R-leap and  $\tau$ -leap.

#### B. CALIBAYES validation

Similar analysis as above is performed on several models in the CaliBayes test suite version DSMTS 21.<sup>17</sup> Three models with solvable mean and standard deviation are tested: the birth-death process, dimerization process, and immigration-death process. Of these a total of nine variations in initial conditions and parameters are simulated (the others not being tested due to limited ER-leap SBML support). The tested models are 1-01, 1-03, 1-04, 1-05, 2-01, 2-02, 2-04, 3-01, and 3-02.

Each test case has 50 time points where  $Z_t$  and  $Y_t$  values

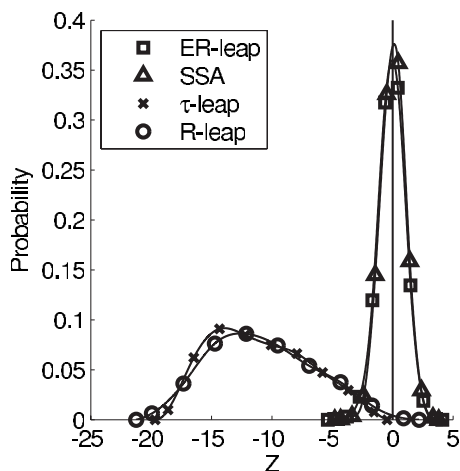


FIG. 2. Distribution of  $Z_i$  for the four algorithms under consideration. ER-leap and SSA demonstrate a standard normal distribution, whereas the approximate methods show  $Z_i$  values far outside the expected range. Reactions  $\{X \rightarrow 2X, X \rightarrow \emptyset\}$  with rate parameters  $\{0.11, 0.1\}$  and  $X(0)=1.0 \times 10^5$ . For ER-leap  $L=30$ . For R-leap  $\theta=0.1$  and  $\varepsilon=0.01$ . For  $\tau$ -leap  $\varepsilon=0.01$ . Each  $Z_i$  calculated from 1000 time points for 1 s intervals up to time  $t=50$ . The number of runs for each method varies in order to get smooth distributions and ranges from  $1.0 \times 10^5$  to  $2.0 \times 10^5$ .

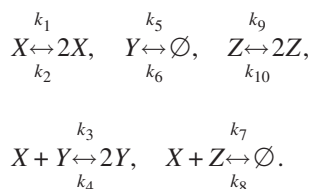
are calculated. A test is considered passing if  $|Z_i| \leq 3.0$  for all 50  $Z_i$  values with one exception per run. Likewise, since the standard deviation normal assumption is not as strong, we require  $|Y_i| \leq 5.0$  for all but one of the  $Y_i$  scores per test. This pass/fail criteria was also suggested in the CALIBAYES documentation.

Furthermore, since the tests are made at discrete time points, a large leap may create a small but nonzero bias if we test at a state preceding the desired time  $t$ . To alleviate this problem we “leap” to a time before  $t$  and then perform small SSA ( $L=1$ ) steps until  $t$  is reached. The SSA steps begin when the time is within  $L\nu/(D+\tilde{D})$  of  $t$ , with  $\nu=7$ . In practice these small steps do not significantly affect running time.

Using the criteria above, we found all tested variations from the CALIBAYES suite to pass, using ER-leap with  $L=3$  or automatically selected  $L$ , and 20 000 simulations per model.

### C. Williamowski–Rössler model

The Williamowski–Rössler model,<sup>18</sup> which contains several bimolecular reactions, is explored to demonstrate the usefulness of the ER-leap algorithm. Results indicate that the approximate methods do not model well the true stochastic behavior for particular instances of the system. Consider the following set of reactions:



We can numerically solve for the corresponding set of deterministic mass action differential equations,

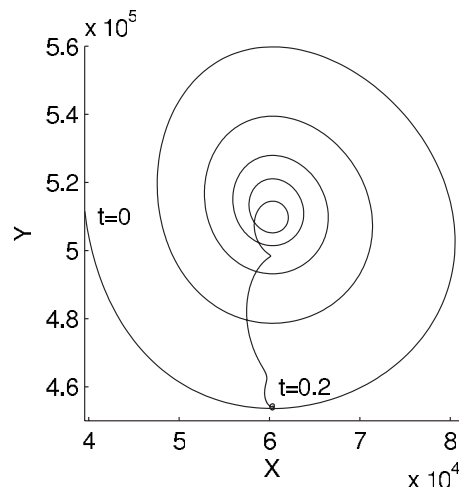


FIG. 3. Mass-action deterministic solution of  $X$  vs  $Y$  from time  $t=0$  to  $t=0.2$  for Williamowski–Rössler model.  $k_1=900$ ,  $k_2=8.3 \times 10^{-4}$ ,  $k_3=0.00166$ ,  $k_4=3.32 \times 10^{-7}$ ,  $k_5=100$ ,  $k_6=18.06$ ,  $k_7=0.00166$ ,  $k_8=18.06$ ,  $k_9=198$ ,  $k_{10}=0.00166$ .  $X(0)=39570$ .  $Y(0)=511470$ .  $Z(0)=0$ .

$$\dot{x} = k_1x - k_3xy - k_2x^2 + k_4y^2 - k_7xz + k_8,$$

$$\dot{y} = k_3xy - k_5y - k_4y^2 + k_6,$$

$$\dot{z} = -k_7xz + k_9z - k_{10}z^2 + k_8,$$

and plot the solution of  $X$  versus  $Y$  as in Fig. 3.

As time progresses the mean trajectory spirals in toward an attraction point near  $\{6.0 \times 10^4, 5.1 \times 10^5\}$ . However, once the inner region is reached, the trajectory falls toward another attraction point around  $\{6.0 \times 10^4, 4.5 \times 10^5\}$ . The stochastic algorithms are run and we can observe the density plots over time for the exact and approximate algorithms in Fig. 4.

As Figs. 4 and 5 demonstrate, there is a substantial difference between the probability densities from the exact and

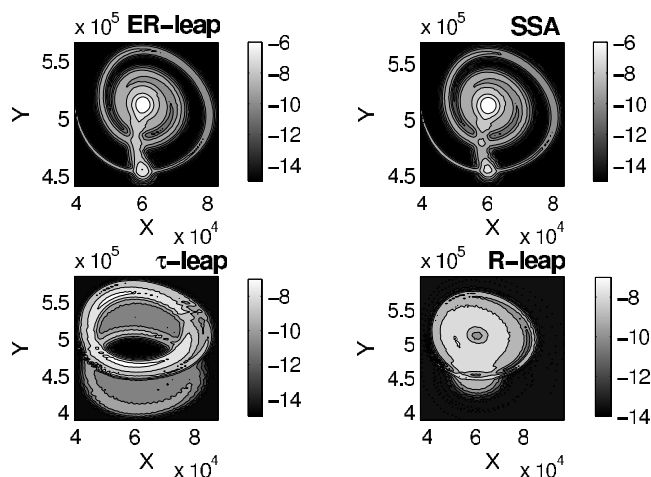


FIG. 4. Comparing log probability densities for various simulation methods over time  $t=0$  to  $t=0.2$ . Same parameters as Fig. 3. SSA and ER-leap appear identical. Total of 1500 samples for each simulator. For ER-leap  $L$  was chosen automatically and averaged  $L=23$ . For  $\tau$ -leap and R-leap  $\varepsilon=0.01$ . For R-leap  $\theta=0.1$ . Measurement taken every  $10^{-4}$  s.



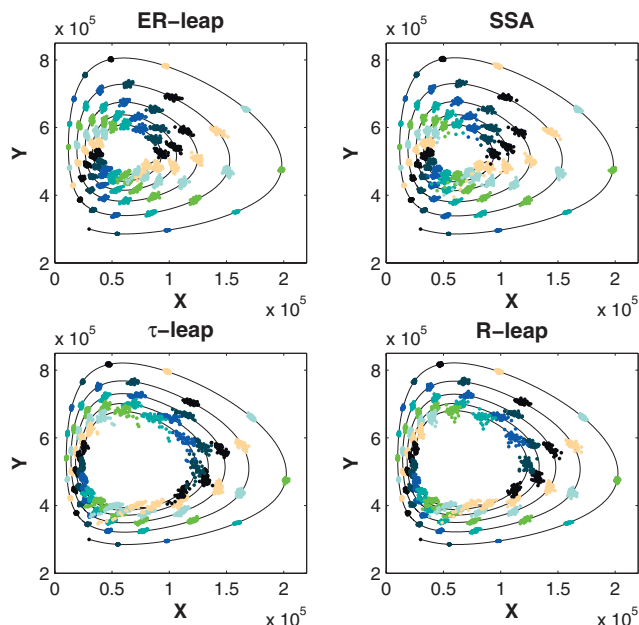


FIG. 5. (Color) Another look at the differences in trajectories. Distribution of 50 runs for the four algorithms. Same network as Fig. 4.  $X(0)=30\,000$ .  $Y(0)=300\,000$ . (so we start further out in the spiral). Simulate from time  $t=0$  to  $t=0.13$ , before the “escape” shown in Fig. 4. A constant amount of time passes between time samples. Each cluster of points represents a group of trajectories that started at the same initial condition and has run for the same amount of time, varying only stochastically, i.e., by the choice of the seed for a random number generator.

approximate simulation methods. However, ER-leap is able to produce an answer similar to that of SSA and is about 4.5 times faster on this example.

We modify the foregoing Williamowski–Rössler model to have rate parameters in the chaotic regime as described in Ref. 18. The idea is that small simulation errors may grow into large errors as time progresses. The SSA mean of  $X$  versus  $Y$  over 1150 runs is shown in Fig. 6. Notice the erratic behavior, which deterministic analysis may have difficulty capturing.<sup>18</sup>

When we examine log densities accumulated over time we observe that ER-leap and SSA have densities that appear very similar, whereas the approximate methods display greater departures from SSA (Figure 7).

In the corresponding mass-action ordinary differential equations in the chaotic regime, small simulation errors grow

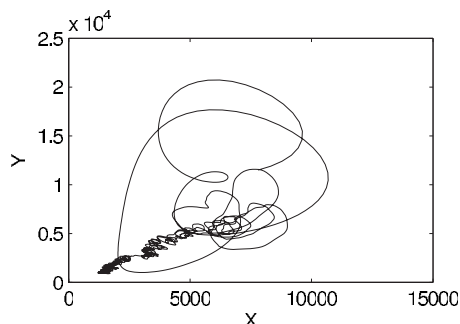


FIG. 6. Mean number of molecules on chaotic system over 1150 SSA runs from time  $t=0$  to  $t=30$ .  $k_1=30$ ,  $k_2=8.3 \times 10^{-4}$ ,  $k_3=0.001\,66$ ,  $k_4=3.32 \times 10^{-7}$ ,  $k_5=10$ ,  $k_6=0.602$ ,  $k_7=0.001\,66$ ,  $k_8=0.602$ ,  $k_9=16.58$ ,  $k_{10}=0.001\,66$ .  $X(0)=7800$ .  $Y(0)=11\,500$ .  $Z(0)=0$ .

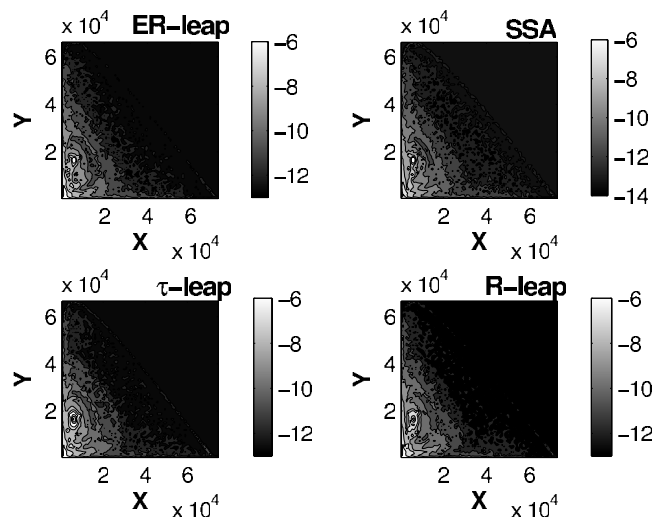


FIG. 7. Comparing  $X$  vs  $Y$  log probability density for various simulation methods over time  $t=0$  to  $t=30$ . Same parameters as in Fig. 6. Total of 1150 samples runs for each simulator. ER-leap  $L$  was chosen automatically and averaged around 11.5. For  $\tau$ -leap and R-leap  $\varepsilon=0.01$ . For R-leap  $\theta=0.1$ . Measurement taken every 0.1 s.

exponentially. Furthermore, mass action analysis has sometimes proven insufficient to model the system even for a large number of molecules.<sup>18</sup> To elucidate model dynamics stochastic simulation methods need to be applied. To our knowledge ER-leap is the fastest such algorithm to do this exactly.

#### D. Scaling of computational cost with reaction events

The acceleration of SSA by ER-leap depends on the number of molecules  $n$  (along with other factors not explored here). We run the Galton–Watson model with initial molecule number  $n$  ranging from 10 to  $9 \times 10^7$  (Fig. 8). As expected the SSA CPU running time scales linearly with  $n$ . The ER-leap CPU time appears to scale as  $O(n^\alpha)$  where  $\alpha$

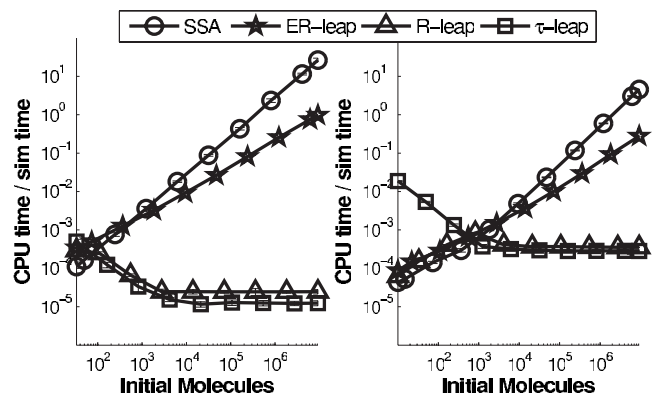


FIG. 8. Log-log scaling of CPU running times for various SSAs. The left panel plot results obtained for the Galton–Watson model with birth rate of 0.101 and death rate of 0.10. Each test is simulated for 30 s. The slope of the ER-leap line is 0.65, and SSA is 0.99, about 1.0 as expected. Ratio is 0.66.  $L$  is chosen automatically for ER-leap. R-leap has accuracy parameters  $\theta=0.1$  and  $\varepsilon=0.01$ .  $\tau$ -leap has parameter  $\varepsilon=0.01$ . The right panel plots results obtained for the dimerization process  $\{2X \rightarrow S, S \rightarrow 2X\}$  with rate parameters  $\{0.001/\nu, 0.01\}$ , respectively, initial values  $S(0)=n$ , singleton molecule  $X(0)=n/2$ , and volume  $\nu=n/100$ . Slope of ER-leap line is 0.58 and slope of SSA line is 0.86 with a ratio of 0.68. Error bars represent one standard deviation.



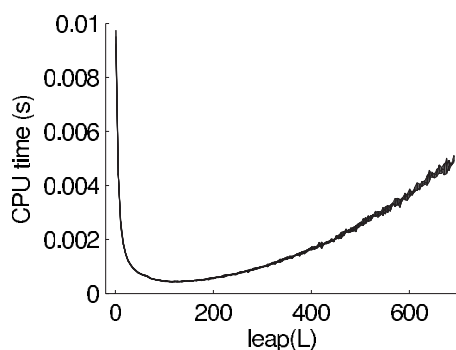


FIG. 9. Varying  $L$  for birth/death process with rate of birth 0.1 and death 0.11.  $X(0)=1 \times 10^7$ .  $X(0)=5 \times 10^6$ . Simulation from  $t=0$  to  $t=5$ . Initially as we increase  $L$ , CPU runtime drops dramatically until the optimum at about  $L=115$  which is about 22 times faster than SSA. For larger  $L$ , the rejection of proposed samples starts to decrease performance and there is a monotonic increase in CPU computation time.

$\approx 2/3$  (Fig. 8). R-leap and  $\tau$ -leap scale much better to large number of molecules, but are not exact algorithms. Notice that the slope of the approximating methods is nearly 0. This is due to the fact that the leap sizes are determined from bounds on relative propensity changes. Because this system only involves first order reactions, this leap control results in sizes that are proportional to  $n$ . Substantial room remains for the improvement of exact algorithms.

Additionally, we can explore the trade-off between the potential gain of large  $L$  and loss of efficiency from rejecting samples from too-ambitious  $L$  values. There is an optimal  $L$  that is model and time specific. We explore this relationship by varying  $L$  for a particular simulation and observing the CPU cost, as plotted in Fig. 9.

This trade-off can also be explored with a log-contour plot of CPU time and  $L$  (Fig. 10). Notice that as simulation time increases, the optimal  $L$  changes. This fact is due to a change in the value of Eq. (21) as reactant numbers change. The lack of multiple local minima in Fig. 10 suggests that dynamic optimization of  $L$  is not a hard problem.

### E. Scaling of computational cost with reaction channels

The acceleration of ER-leap over SSA is explored as a function of the number of reaction channels. The

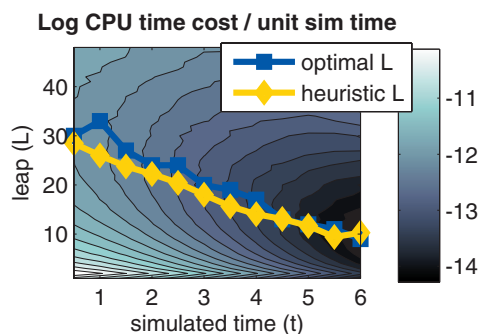


FIG. 10. (Color) ER-leap contour plot of log CPU time per unit simulation time vs simulation time and leap size  $L$ . Overlay of optimal and heuristic choice of  $L$  (from one run). Notice that the optimal leap  $L^*$  changes during simulation from  $L^*=34$  at  $t=0$  to about  $L^*=8$  at  $t=6$ . Basic cascading network  $\{S1 \rightarrow S2, S2 \rightarrow S3, S3 \rightarrow S4\}$  and all rates of 1.0. Initial values:  $S1=4.2 \times 10^4$ ,  $S2=4.0 \times 10^4$ ,  $S3=3.5 \times 10^4$ , and  $S4=0$ . Results averaged over 500 runs.

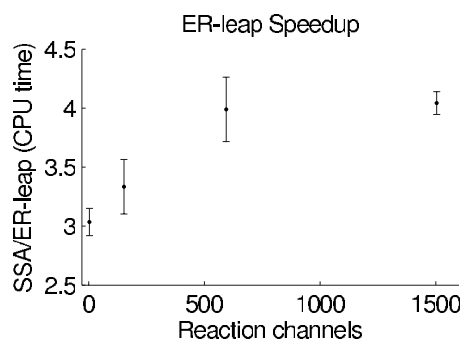


FIG. 11. Speedup is calculated as SSA wall clock time divided by ER-leap wall clock time. It increases monotonically from a one-cell system with ten reaction channels to a  $4 \times 4 \times 4$  grid with 1504 reaction channels. In ER-leap  $L$  was chosen automatically, and averaged 23 over all experiments. Error bars are one standard deviation. Same rate parameters as Fig. 3. Rate of diffusion is 0.01 and the initial number of molecules in each cell  $X(0)=5.0 \times 10^4$ ,  $Y(0)=4.5 \times 10^5$ ,  $Z(0)=3.0 \times 10^4$ .

Williamowski–Rössler model is replicated over a  $d$ -dimensional grid. In each compartment of the grid there is a copy of the Williamowski–Rössler reaction network, including all of its chemical species and their intracompartamental reactions. In addition, molecules diffuse (stochastically) between adjacent grid compartments. This is accomplished by replicating all WR reactions over the set of compartments, and adding new reactions of the form  $\{X_c \xrightarrow{\rho} X_{c'}\}$  where  $c$  is the grid coordinate for molecules of type  $X$  and  $c'$  is any neighboring compartment. Diffusion is to adjacent compartments only, so the  $L_1$  distance between  $c$  and  $c'$  is 1. In the experiments shown,  $d=3$ . As Fig. 11 demonstrates, ER-leap may be used to accelerate systems with many reaction channels. It also demonstrates the feasibility of applying ER-leap to spatially structured models.

Although the three-dimensional grid of compartments simulated here results in efficient simulation on a relatively highly connected network of reactions and reactants, with a graph diameter proportional to the cube root of the number of nodes, the ER-leap algorithm could be stressed to the point of inefficiency by other topologies. For example, a fully connected (diameter one) compartment graph, or a scale-free (logarithmic or sublogarithmic diameter) compartment graph, each have much higher connectivity than was tested here. Further work will be required to evaluate and possibly adapt the ER-leap algorithm for such alternative large-scale network structures.

### IV. CONCLUSIONS

We have derived an exact accelerated algorithm for stochastic simulation of chemical reactions, using rejection sampling together with upper and lower bounds on the probability of an outcome of a run of  $L$  reactions. We have demonstrated a speedup to sublinear time for simulating a large number of reaction events. We have verified the accuracy of the method with sensitive tests including examples from the CALIBAYES test suite and a chaotic reaction network.

We note that the SSA has also been accelerated, without approximation, by executing one reaction event at a time, lowering the cost of sampling each reaction event when there

are many possible reactions to choose from.<sup>19</sup> An alternative acceleration of SSA has been proposed<sup>20</sup> based on exploiting cycle structure. The present ER-leap algorithm is based on the R-leap algorithm<sup>11</sup> that accelerates the SSA by efficiently executing a number of reaction firings together. ER-leap offers an acceleration that is more general than the efficient sampling of many reaction channels or types<sup>19</sup> or the exploitation of cycles.<sup>20</sup> Instead, like an approximate acceleration scheme, it exploits the scaling possible for large numbers of reactant particles (molecules) and of reaction events. In these conditions, and for reaction networks (such as the Williamowski–Rossler oscillator) for which high-accuracy or exact simulation is necessary to find the correct long-time behavior, ER-leap may turn out to be the currently preferred algorithm. In any case, the existence of ER-leap demonstrates that it is possible to create exact, accelerated SSA which scale better than SSA with respect to the number of reactant particles and reaction events. Among these exact methods, only ER-leap has been demonstrated to have an asymptotically sublinear (roughly 2/3 power of SSA) simulation time as a function of the number of reaction events for a regular family of simulation problems, namely two exactly solvable networks (Galton–Watson and dimerization) in a test suite for SSAs.

Future work includes the hybridization of the present ER-algorithm with techniques from other exact simulation algorithms that more directly address scaling with the number of reaction channels, as well as improvements in the extension of the ER algorithm to spatially dependent stochastic simulations. The numerical experiments of Sec. III E, along with previous work such as the use of tau-leap<sup>21</sup> and R-leap<sup>22</sup> in spatial models, show the feasibility of spatial stochastic simulations but do not, we think, exhaust the avenues for their acceleration.

Software for the ER-leap algorithm is provided at <http://computableplant.ics.uci.edu/erleap>.

## ACKNOWLEDGMENTS

E.M. wishes to thank ETH and Professor Joachim Buhman for supporting a visit to ETH Zürich. Other support was provided by NSF's Frontiers in Biological Research (FIBR) program Award No. EF-0330786, and NIH P50-GM76516.

<sup>1</sup>D. T. Gillespie, *J. Phys. Chem.* **81**, 2340 (1977).

<sup>2</sup>F. T. Gillespie, *J. Chem. Phys.* **115**, 1716 (2001).

<sup>3</sup>A. Chatterjee, K. Mayawala, J. S. Edwards, and D. G. Vlachos, *Bioinformatics* **21**, 2136 (2005).

<sup>4</sup>Y. Cao, D. T. Gillespie, and L. R. Petzold, *J. Chem. Phys.* **123**, 054104 (2005).

<sup>5</sup>Y. Cao, D. T. Gillespie, and L. R. Petzold, *J. Chem. Phys.* **124**, 044109 (2006).

<sup>6</sup>E. Weinan, D. Liu, and E. V. Eijnden, *J. Chem. Phys.* **123**, 194107 (2005).

<sup>7</sup>A. Samant and D. G. Vlachos, *J. Chem. Phys.* **123**, 144114 (2005).

<sup>8</sup>H. Salis and Y. N. Kaznessis, *J. Chem. Phys.* **123**, 214106 (2005).

<sup>9</sup>Y. Cao, D. T. Gillespie, and L. R. Petzold, *J. Chem. Phys.* **122**, 014116 (2005).

<sup>10</sup>A. Slepoy, A. P. Thompson, and S. J. Plimpton, *J. Chem. Phys.* **128**, 205101 (2008).

<sup>11</sup>A. Auger, P. Chatelain, and P. Koumoutsakos, *J. Chem. Phys.* **125**, 084103 (2006).

<sup>12</sup>N. G. Van Kampen, *Stochastic Processes in Physics and Chemistry*, 3rd ed. (North-Holland, Amsterdam, 2007).

<sup>13</sup>G. Yosiphon and E. Mjolsness, *Learning and Inference in Computational Systems Biology* (MIT, Cambridge, 2008), <http://computableplant.ics.uci.edu/papers/>.

<sup>14</sup>D. J. Wilkinson, *Stochastic Modelling for Systems Biology (Mathematical and Computational Biology)* (Chapman and Hall, London/CRC, Boca Raton, 2006).

<sup>15</sup>E. Mjolsness and G. Yosiphon, *Annals of Mathematics and Artificial Intelligence* **47**, 329 (2006).

<sup>16</sup>J. von Neumann, *Various Techniques Used in Connection with Random Graphs* (U.S. Government Printing Office, Washington, 1951), pp. 36–38.

<sup>17</sup>T. W. Evans, C. S. Gillespie, and D. J. Wilkinson, *Bioinformatics* **24**, 285 (2008).

<sup>18</sup>H. Wang and Q. Li, *J. Chem. Phys.* **108**, 7555 (1998).

<sup>19</sup>M. A. Gibson and J. Bruck, *J. Phys. Chem. A* **104**, 1876 (2000).

<sup>20</sup>M. D. Riedel and J. Bruck, <http://paradise.caltech.edu/papers/etr077.pdf>

<sup>21</sup>D. Rossinelli, B. Bayati, and P. Koumoutsakos, *Chem. Phys. Lett.* **451**, 136 (2008).

<sup>22</sup>K. P. Bayati and P. Chatelain, *Phys. Chem. Chem. Phys.* **10**, 5963 (2008).